LA-UR- 96-3096

CONF-960994--8

Title: EROSION OF THIN CARBON FOILS BY 20 KEV AND 40 KEV Ar+ BOMBARDMENT

Author(s): Herbert O. Funsten
Mark Shappirio

Submitted to: Nuclear Instruments and Methods
Proceedings of the IBMM Conference
Albuquerque, New Mexico
September 2-6, 1996

DISTRIBUTION OF THIS DOCUMENT IS UNLIMITED

Los Alamos
NATIONAL LABORATORY

Form No. 836 R5
ST 2629 10/91

Erosion of thin carbon foils by 20 keV and 40 keV Ar^+ irradiation

H.O. Funsten and M. Shappirio

Los Alamos National Laboratory

Los Alamos, NM 87545

Abstract

Nominal 2 $\mu g/cm^2$ carbon foils were irradiated with 20 keV and 40 keV Ar^+ ions at fluences of up to $1.1x10^{16}$ Ar^+/cm^2. The foil erosion, which was determined by measuring changes in the angular scatter distribution of 2 keV protons transiting the foil, is observed to reach a constant rate of 3.5 C atoms removed per incident Ar^+. The independence of the sputter yield on foil thickness indicates that interactions leading to sputtering occur within a depth of 0.5 $\mu g/cm^2$ of the sputter surface. Using theoretical and TRIM estimates for the backward sputtering yield, the transmission sputtering yield is a factor of 3-16 times larger than the backward sputtering yield. The fraction of holes created in the foil by Ar^+ irradiation linearly increases with fluence above a fluence of $4x10^{15}$ Ar^+/cm^2, and the foil lifetime is $8.7x10^{15}$ Ar^+/cm^2.

Corresponding Author:
Herbert Funsten
MS D466
Los Alamos National Laboratory
Los Alamos, NM 87545

Phone: (505)665-4314
FAX: (505)665-7395
email: hfunsten@lanl.gov

1. Introduction

Thin carbon foils are used extensively in particle diagnostic instrumentation, for example as secondary electron emitters in time-of-flight (TOF) mass spectrometry and for charge modification of ions or neutral atoms [1,2]. In these applications, particle energies are typically < 100 keV, and quantification of radiation-induced damage in this energy regime is necessary to characterize instrument performance.

Thin carbon foils are routinely used as charge stripping targets in accelerators. At MeV beam energies, physical radiation-induced damage such as foil thickening, shrinkage, and tearing has been clearly observed [3-6]. The origin of this damage has been attributed to hydrocarbon cracking, radiation-induced chemical effects, and defect accumulation [3,6-9]. At MeV energies, in which the nuclear stopping power is much less than the electronic stopping power, sputtering plays only a small role in damage to the foils [6].

At keV energies, in which the nuclear stopping power is larger than the electronic stopping power, foil erosion by sputtering is a major contributor to foil damage. In this study, we examine erosion of thin carbon foils by 20 and 40 keV Ar^+ irradiation and quantify hole formation in the foils that degrades instrumentation performance.

2. Experimental Apparatus

Fig. 1 illustrates the experimental apparatus used to study foil erosion. A monoenergetic, mass-analyzed ion beam was directed through a 0.64 cm aperture (aperture A1) and onto a foil target, which was surrounded by a secondary electron suppression can biased to -200 V to ensure an accurate measurement of the ion current incident on the foil. Nominal 2 $\mu g\ cm^{-2}$ carbon foils

were mounted on a 333 line-per-inch Ni grid. Close behind the mounted foil was a 1 mm diameter aperture (aperture A2).

As will be described in Section 3, the foil thickness was measured by comparing the measured scatter distribution of 2 keV protons that transit the foil to a theoretical scattering model. The scatter distribution was measured by rotating the foil target 180^0 so that the protons transited aperture A2 before striking the foil, and then acquiring the scatter distribution using a position sensitive imaging microchannel plate (IMCP) detector located 5.1 cm from the foil.

Intermittently during Ar^+ irradiation of the foil, a scatter distribution of 2 keV protons was acquired to determine the thickness change resulting from the Ar^+ irradiation. The Ar^+ beam current on the foil target, which was measured every second, was typically 30 nA, and the Ar^+ fluence Φ was determined by integrating the beam current over the irradiation time. Aperture A1 was used to uniformly bombard a large area of the foil so that the measurement of the scatter distribution using the smaller aperture A2 represented a uniformly bombarded region of the foil.

3. Foil thickness and hole fraction measurements

The foil thickness was derived by measuring the angular scattering halfwidth $\psi_{1/2}$ and calculating a thickness using scattering theory. The measured scatter distribution $S(\psi)$ is fit to [10]

$$S(\psi) = S_0 \left(1 + \frac{\psi^2}{2\, b\, \sigma^2} \right)^{-b} \qquad (1)$$

where S_0 is the distribution maximum, ψ is the scatter angle, σ describes the distribution width, and b is a weight parameter describing the tail width. The scattering halfwidth at half maximum of this distribution is

$$\psi_{1/2} = \sigma\left(2b\left(2^{1/b}-1\right)\right)^{-b} \quad . \tag{2}$$

Fig. 2 shows the measured normalized angular scatter distributions (points) of 2 keV protons before and after irradiation by Ar^+. The scatter distribution after Ar^+ irradiation consists of the sum of two distributions: the angular scatter distribution from protons transiting hole-free regions of the foil and a high count region, called the hole distribution, in the central region resulting from protons passing unscattered through holes in the foil [11,12]. The solid lines, which are fits to the scatter distributions using Eq. 1, agree well with the data.

From multiple small-angle scattering theory [13,14], we represent angular scattering of a projectile by a foil using reduced units. The reduced scattering halfwidth is

$$\Psi_{1/2} = \psi_{1/2}\,\frac{\varepsilon}{2}\,\frac{m_1+m_2}{m_2} \tag{3}$$

where m is the atomic mass and the subscripts 1 and 2 refer to the projectile and target, respectively. The reduced energy is

$$\varepsilon = \frac{a\,E\,m_2}{Z_1\,Z_2\,e^2(m_1+m_2)} \qquad (4)$$

where the Thomas-Fermi screening parameter a equals $a_0(Z_1^{2/3}+Z_2^{2/3})^{-1/2}$, a_0 is the Bohr radius, Z is the atomic number, E is the particle energy, and e is the electron charge. The reduced thickness is

$$\tau = \pi a^2 N t \qquad (5)$$

where N is the atomic density of the foil and t is the foil thickness.

To obtain a foil thickness from the scattering distribution, we calculate $\Psi_{1/2}$ from the measured $\psi_{1/2}$ using Eq. 3, determine the corresponding reduced thickness τ from the function $\Psi_{1/2}(\tau)$ derived from the scatter theory [13,14], and obtain t using Eq. 5. Derivation of the foil thickness assumes a foil composition of carbon.

As the Ar^+ beam erodes the foil, holes are created. These holes can degrade the performance of a thin foil used for charge modification or secondary electron emission, e.g., as in foil-based TOF mass spectrometry. The fraction of holes in the area bombarded by protons is defined as $f_H = (\Sigma_{TOT} - \Sigma_{FIT})/\Sigma_{TOT}$ where Σ_{TOT} is the total number of counts in the measured scatter distribution and Σ_{FIT} equals the total counts in the fit of Eq. 1 to the tails of the scatter distribution, i.e., with the central region containing the hole distribution removed.

4. Results and Discussion

Fig. 3 shows the foil thickness t as a function of the Ar^+ fluence Φ. For both 20 keV and 40 keV Ar^+ irradiation, t initially decreases rapidly until $\Phi \approx 10^{15}$ Ar^+/cm^2, and then decreases linearly with increasing fluence. The rapid initial decrease of t likely results from sputtering of adsorbed species and residue from the parting agent used to mount the foil. The adsorbate and residue are easily sputtered since they are lightly bound to the foil. Furthermore, they contain heavier atomic species than C which causes larger angular scattering of the 2 keV protons and therefore overestimates the foil thickness that was derived assuming a composition of C only.

For $\Phi \geq 10^{15}$ Ar^+/cm^2, the foil is eroded at a constant rate, as illustrated by the dotted and dashed lines which are fits to the data for which $\Phi \geq 10^{15}$ Ar^+/cm^2. Extrapolation of these fitted lines to $\Phi = 0$ indicates that the initial carbon foil thicknesses are 25% and 36% less than the nominal value of 2 $\mu g/cm^2$ cited by the manufacturer. The erosion rate for both 20 keV and 40 keV Ar^+ irradiation is approximately 0.07 $\mu g/Ar^+$, which corresponds to a total sputter yield of Y = 3.5 carbon atoms per incident Ar^+.

We now investigate the variation in sputtering from the entrance (backward sputtering) and exit (transmission sputtering) surfaces of the foil. The total sputter yield Y consists of the sum of the backward sputter yield Y_B and the transmission sputter yield Y_T, i.e., $Y = Y_B + Y_T$. For 20-40 keV Ar^+ irradiation of C, sputtering theory predicts $Y_B = 0.9$ [15], while TRIM [16] predicts $Y_B = 0.2$. Based on these estimations and using Y = 3.5, Y_T likely lies within the range of 2.6 to 3.3 and the ratio Y_T / Y_B ranges from 3 to 16. This enhancement transmission sputtering yield is expected since transmission sputter consists primarily of recoil atoms, which preferentially have a velocity in the direction of the incident beam [15,17].

As previously stated, the erosion rate for 20 keV Ar^+ irradiation decreases linearly with increasing Φ for $\Phi \geq 10^{15}$ Ar^+/cm^2. This linearity indicates that the sputter yield is independent of the thickness, and backward and transmission sputtering can be treated independently as sputtering from semi-infinite slabs. Since this linear dependence is observed down to a foil thickness of 0.5 $\mu g/cm^2$, the upper bound for both the range of the recoils in the foil and the depth of the energy density function [15,17] from which sputtering originates is 0.5 $\mu g/cm^2$.

Figure 4 shows the hole fraction f_H of the region bombarded by 2 keV protons as a function of Φ. Significant formation of holes does not occur until a threshold fluence of $\Phi \approx 4.5 \times 10^{15}$ Ar^+/cm^2. Above this threshold, the hole fraction increases linearly with increasing Φ for both 20 keV and 40 keV Ar^+ irradiation. After a dose of $\Phi \approx 10.7 \times 10^{15}$ Ar^+/cm^2, at least 73% of the foil contains holes. While the observed holes in the foil could result from erosion of thin regions of the foil, they could also be formed by structural changes in the foil resulting in localized foil tearing similar to tearing is observed from MeV irradiation [6,9].

The foil lifetime, defined here as the fluence $\Phi_{1/2}$ corresponding a hole fraction $f_H = 0.5$, is $\Phi_{1/2} = 8.7 \times 10^{15}$ Ar^+/cm^2. This compares to the foil lifetime resulting from 1.2 MeV Ar^+ irradiation of a 5 $\mu g/cm^2$ carbon foil of $\Phi_{1/2} = 10^{17}$ Ar^+/cm^2 [7].

In summary, we have quantified damage to 2 $\mu g/cm^2$ carbon foils by 20 keV and 40 keV Ar^+ irradiation. A constant sputter yield of 3.5 is observed and indicates that the sputter process originates within a depth in the foil of 0.5 $\mu g/cm^2$. The transmission sputter yield is 3 to 16 times larger than the backward sputter yield. The creation of holes in the foil is a apparently a threshold phenomena, and the rate of hole formation is observed to increase linearly with increasing Ar^+ fluence.

Acknowledgments: The authors gratefully acknowledge the laboratory assistance of M. Vigil, J. Baldonado, and D. Everett. This work was performed under the auspices of the United States Department of Energy.

References

[1] D.J. McComas, J.E. Nordholt, S.J. Bame, B.L. Barraclough, and J.T. Gosling, Proc. Natl. Acad. Sci. USA 87 (1990) 5925.

[2] H.O. Funsten, D.J. McComas, and B.L. Barraclough, Opt. Eng. 32 (1993) 3090.

[3] J.L. Yntema, IEEE, Trans. Nucl. Sci. NS-23 (1976) 1133.

[4] A.E. Livingston, H.G. Berry, and G.E. Thomas, Nucl. Instr. and Meth. 148 (1978) 125.

[5] D. Ramsey, Nucl. Instr. and Meth. 167 (1979) 41.

[6] G. Dollinger and P. Maier-Komor, Nucl. Instr. and Meth. A 282 (1989) 223.

[7] E.A. Koptelov, S.G. Lebedev, and V.N. Panchenko, Nucl. Instr. and Meth. A 256 (1987) 247.

[8] T. Wang, W. Wang, and B.Chen, Nucl. Instr. and Meth. B 71, (1992) 186

[9] S.G. Lebedev, Nucl. Instr. and Meth. B 85 (1994) 276.

[10] M. Oetliker, Thesis, University of Bern, Switzerland (1989).

[11] H.O. Funsten, D.J. McComas, and B.L. Barraclough, Nucl. Instr. and Meth. B66 (1992) 470.

[12] H.O. Funsten, B.L. Barraclough, and D.J. McComas, Rev. Sci. Instrum. 63 (1992) 4741.

[13] L. Meyer, Phys. Status Solidi B 44 (1971) 253.

[14] P. Sigmund and K.B. Winterbon, Nucl. Instr. and Meth. 199 (1974) 541.

[15] H.H. Andersen and H.L. Bay, in Sputtering by Particle Bombardment I, Ed. R. Bahrisch (Springer, Berlin, 1981) 145-256.

[16] TRIM Computer Code, J.F. Ziegler, J.P. Biersack, and U. Littmark, The Stopping and Range of Ions in Solids, Vol. 1 (Permagon, New York, 1985) p. 53.

[17] P. Sigmund, Phys. Rev. 184 (1969) 383.

Figure Captions

Fig. 1. The experimental apparatus consisted of beam-defining apertures, a foil target within a secondary electron suppression can, and an imaging microchannel plate detector. The foil was irradiated with 20 keV and 40 keV Ar^+. For the angular scatter measurement of 2 keV protons, from which the foil thickness is calculated, the foil target was rotated 180^0, and the proton beam transited aperture A2 before striking the foil.

Fig. 2. The normalized angular scatter distributions of incident 2 keV protons after $\Phi = 0$ and $\Phi = 7.4 \times 10^{15}$ Ar^+/cm^2 show an initial hole-free foil and, after irradiation by Ar^+, a large fraction of holes in the foil as indicated by the presence of the hole distribution. The solid lines are fits of Eq. 1 to the scattered proton data.

Fig. 3. The foil thickness, derived from the angular scatter distribution of 2 keV protons, is depicted as a function of the Ar^+ fluence. For $\Phi > 10^{15}$ ions/cm^2, a sputter yield of 3.5 C atoms per incident Ar^+ is observed for both 20 keV Ar^+ (triangles) and 40 keV Ar^+ (squares).

Fig. 4. The fraction of the foil consisting holes is depicted as a function of ion fluence. The rate of hole formation for $\Phi > 4 \times 10^{15}$ ions/cm^2 is similar for both 20 keV and 40 keV Ar^+. The dashed line represents a linear fit of $f_H(\Phi)$ to Φ for $\Phi > 4.5 \times 10^{15}$ ions/cm^2.

Funsten and Shappirio, Fig. 1

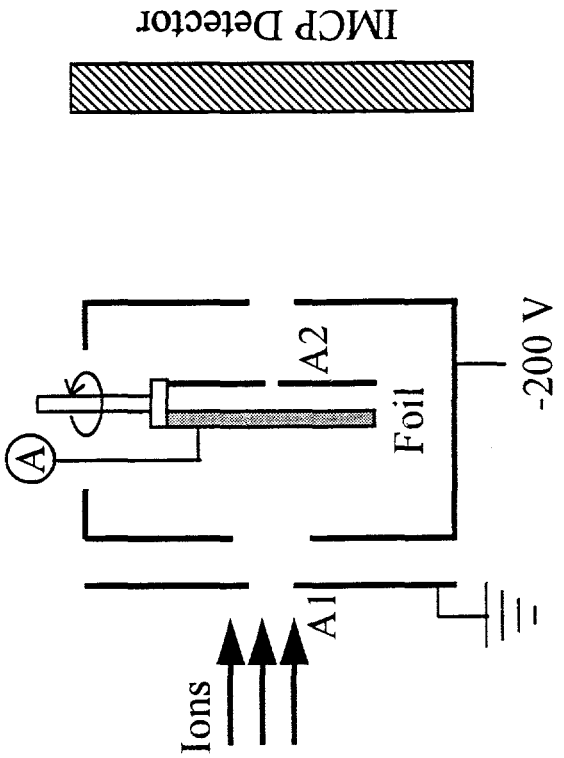

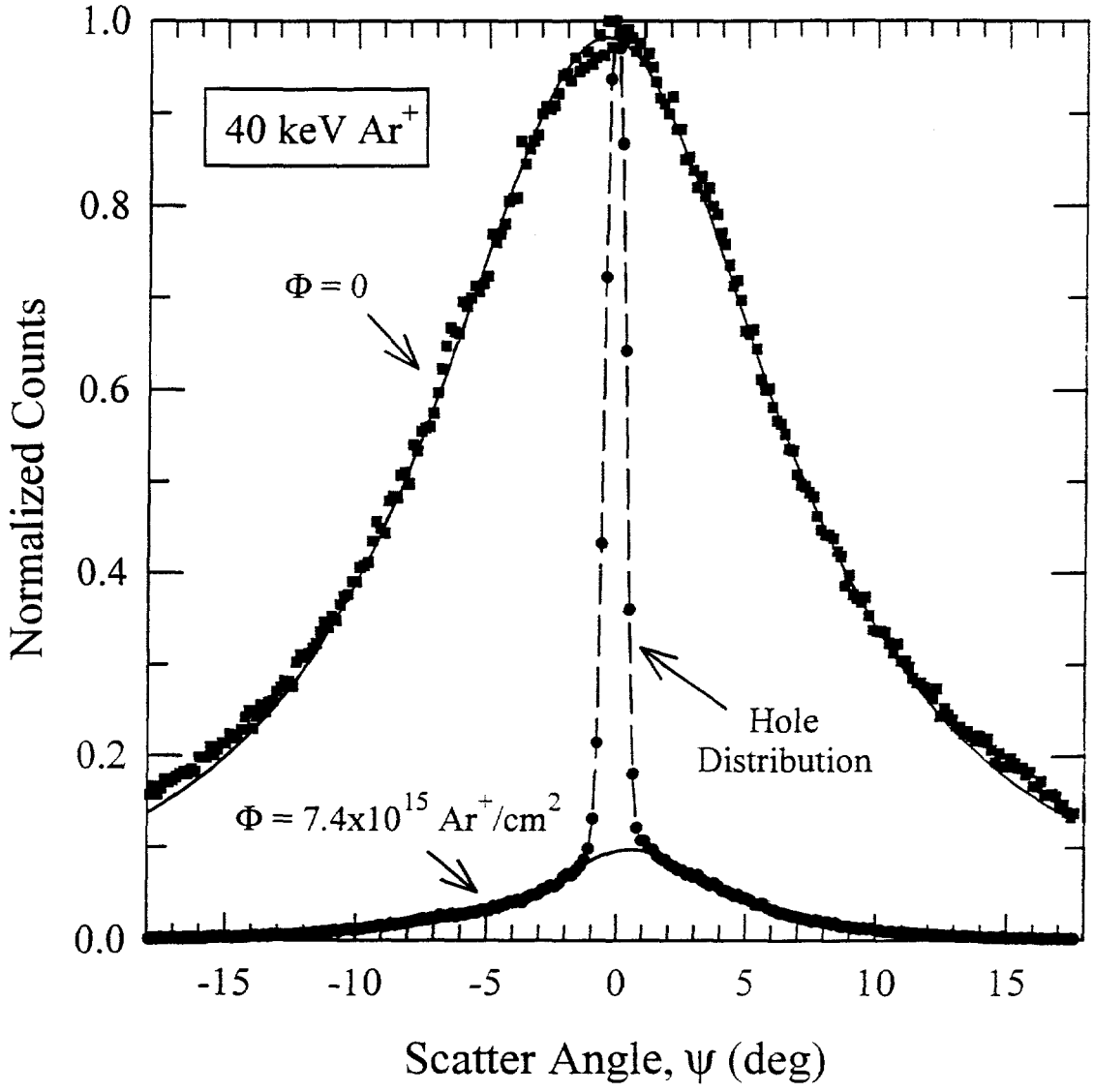
40 keV Ar+
Φ = 0
Hole
Distribution
Φ = 7.4x10^15 Ar+/cm^2
Normalized Counts
Scatter Angle, ψ (deg)
1.0
0.8
0.6
0.4
0.2
0.0
-15
-10
-5
0
5
10
15

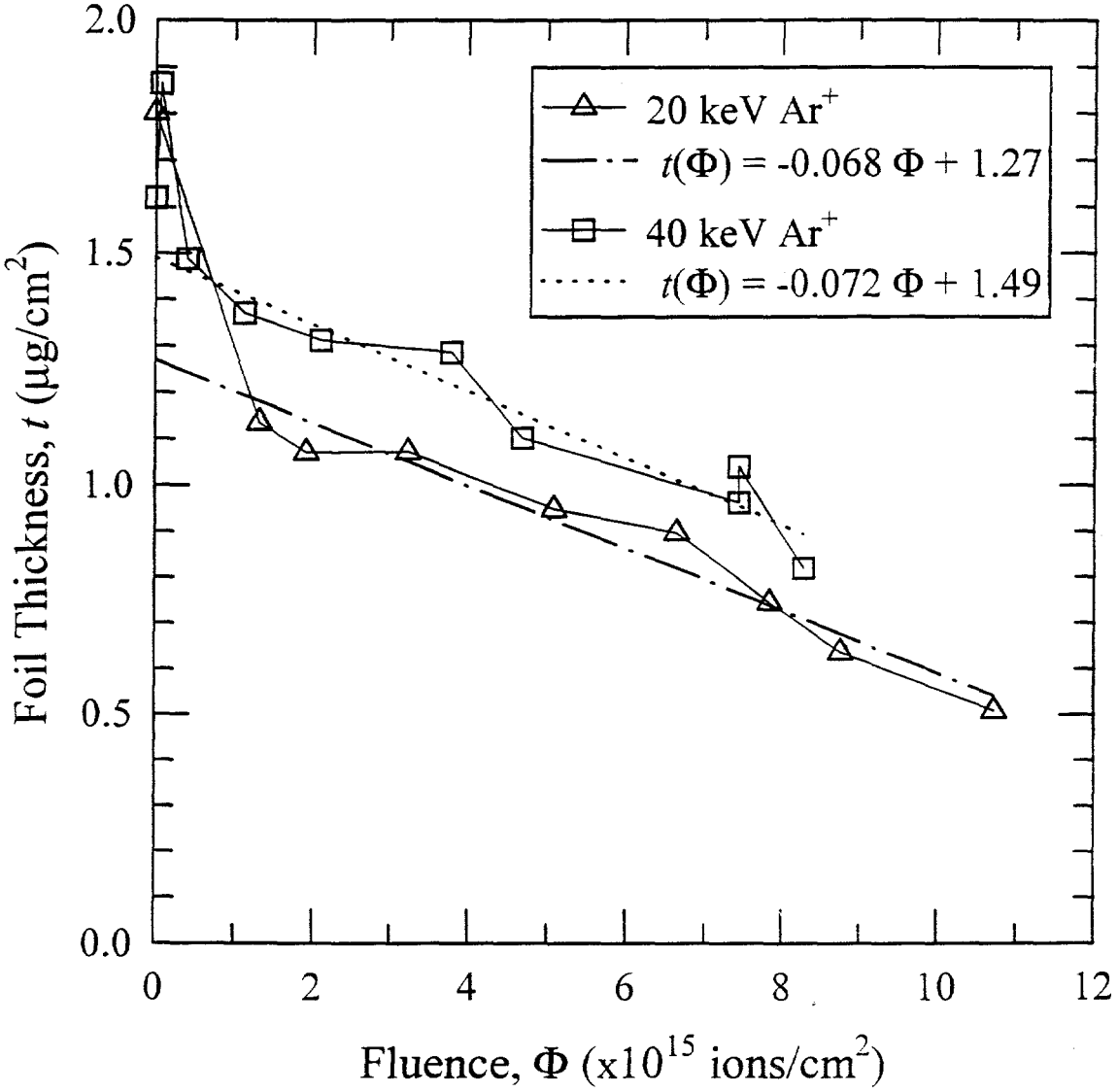
2.0
1.5
1.0
0.5
0.0
0
2
4
6
8
10
12
Foil Thickness, t (μg/cm²)
Fluence, Φ (x10¹⁵ ions/cm²)
20 keV Ar⁺
t(Φ) = -0.068 Φ + 1.27
40 keV Ar⁺
t(Φ) = -0.072 Φ + 1.49